

# Characterization of a high Reynolds number turbulent boundary layer by means of PIV

JM Foucaut<sup>1\*</sup>, C Cuvier<sup>1</sup>, J. Soria<sup>2</sup> and C Willert<sup>3</sup>

<sup>1</sup> Univ. Lille, CNRS, ONERA, Arts et Métiers ParisTech, Centrale Lille, FRE CNRS 2017-LMFL-  
Laboratoire de Mécanique des Fluides de Lille-Kampé de Fériet F-59000, Lille, France

<sup>2</sup> Monash University, LTRAC, Department of Mechanical and Aerospace Engineering,  
Clayton Campus, Melbourne, Australia

<sup>3</sup> DLR Institute of Propulsion Technology, Köln, Germany

\*[jean-marc.foucaut@centralelille.fr](mailto:jean-marc.foucaut@centralelille.fr)

## Abstract

To characterize the turbulent boundary layer evolution in the LMFL wind tunnel, two experiments of velocity measurement by PIV were carried out. A first campaign was done based on a high magnification 2C2D PIV in the near wall region in order to capture the near wall scales and the mean gradient. A second experiment of stereo PIV using two systems was carried out to measure the full boundary layer with a good spatial resolution. By merging these two experiments, a good characterization can be made at 3 stations along the wind tunnel and for three free-stream velocities.

## 1 Introduction

Since the study of Klebanoff and Diehl (1951), the zero-pressure-gradient (ZPG) turbulent boundary layer (TBL) is one of the most investigated wall bounded flow. High accuracy ZPG TBL data are of great importance for highlighting the influence of new parameters such as roughness, pressure gradient, etc.. However, the true statistics of a ZPG TBL is still often subject to controversies and this is particularly true at high Reynolds numbers (Marusic, et al., 2010). The first point of discrepancy is that it is often difficult to compare accurately the different experimental conditions. Comparisons of previous experimental data sets have shown significant discrepancies between different studies even if the Reynolds number were the same ((Chauhan, et al., 2009), (Laval, et al., 2017)). The quality of the flow is also of importance as external turbulence level or pressure gradient close to zero can affect the comparison. The classical way to compare is to use a judicious scaling and to match the Reynolds numbers. In this case, the difference can come from the accuracy of the measurement of the statistics, which is generally good, but also of the scaling parameter such as the friction velocity, which is used to normalize the profiles in the inner region.

In the present study, the statistics are measured in the TBL wind tunnel of Lille for three infinite velocities and three streamwise stations in order to obtain nine profiles with a large range of Reynolds numbers. Several profiles are also obtained at the same Reynolds number. This experiment was possible thanks to the extension of the transparent test section and the temperature and velocity regulation of the wind tunnel. The measurement was done by PIV. The accuracy is obtained by using several magnifications depending on the wall distance.

## 2 Experimental setup

In a turbulent boundary layer, the mean streamwise velocity gradient increases strongly as  $1/y$  where  $y$  is the wall distance. Moreover, the turbulence level increases down to 15 wall-units and after decreases to 0 at the wall (Marusic, et al., 2010). Such a distance corresponds to about 0.1% of the boundary layer thickness  $\delta$ . The turbulent scales are proportional to  $y$  up to about 30% of  $\delta$  (Townsend, 1976), (Srinath, et al., 2018)). In order to both capture the strong gradient and to limit the filtering of scales, two PIV experiments with two different magnifications were carried out in the LMFL boundary layer wind tunnel. The advantage of this facility are both the dimensions, a 20 m long test section fully transparent 2 m wide and 1 m in height and a relatively low velocity (maximal free-stream velocity  $U_\infty = 9$  m/s). Such characteristics allow the generation and study of a thick boundary layer (about 24 cm at the end of the test section) at high Reynolds number. This facility has been designed for intensive use of optical metrology. In the following,  $x$  is the streamwise axis,  $y$  the wall normal one and  $z$  is spanwise.

The first experiment is a streamwise wall-normal 2C2D set-up composed of a sCMOS camera equipped with a 300 mm lens to obtain a magnification of 0.43 (field of view of 32 mm along  $x$  and 33 mm along  $y$  located at the wall) at 1.03 m working distance (extension tube of 140 mm). The  $f\#$  number was set at 8 to obtain particle image size of about 2 px to optimize the accuracy (Foucaut, et al., 2003) and a displacement of about 20 px in the upper part of the field of view was selected to obtain a high dynamic range of the turbulence. Also, to be sure of good convergence statistics, 10000 fields were recorded. The light sheet thickness was 0.3 mm. Figure 1 shows a picture of the experimental set-up where you can see the specific arrangement of the length. The images were processed with the modified version of MatPIV at LMFL. The analysis was done with a multipass approach (Willert & Gharib, 1991), (Soria, 1998)) ending with  $24 \times 24$  interrogation window size (corresponding to 0.36 mm  $\times$  0.36 mm or about 8 wall-units at the highest Reynolds number) which was selected to be a good compromise between noise and filtering. Before the final pass, image deformation was used to improve the capture of the gradient and thus the quality of the data (Scarano, 2002), (Lecordier & Trinité, 2004)).

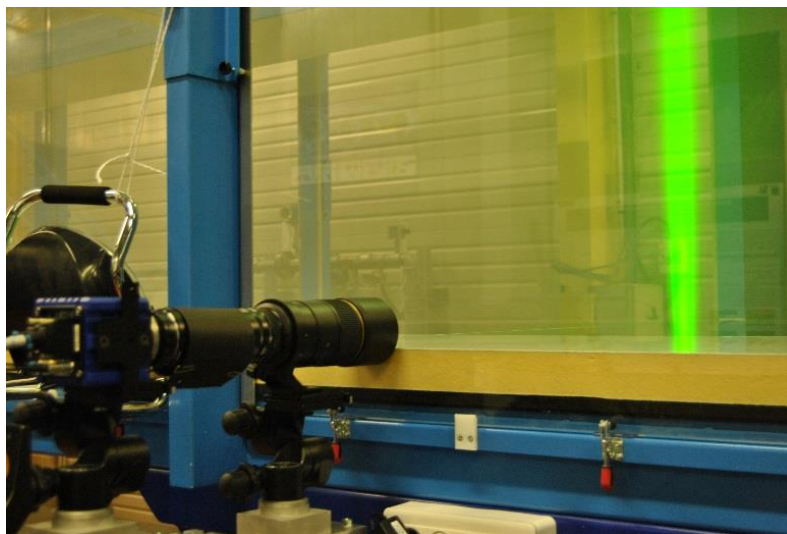


Figure 1 : Picture of the 2C2D set-up

The second experiment is made by a double stereo PIV (3C2D) setup composed of four sCMOS cameras equipped with 135 mm lenses at  $f\#$  8 in order to obtain a large field and keep a good spatial resolution. The field of view obtained is 26.5 cm and 32 cm in wall normal and streamwise direction, respectively, in order to obtain the full boundary layer properties (magnification of 0.083). The displacement was set at about 13 pixels at the top of the field of view and 10000 fields were also recorded to ensure good turbulence statistics. The light sheet thickness was 0.6 mm. The reconstruction used is the one proposed by Soloff et al. (1997) and a self-calibration similar to Wieneke (2005) was applied. The analysis was also done with MatPIV with

a multipass approach. The final interrogation window size was  $18 \times 24$  (corresponding to  $1.9 \text{ mm} \times 1.9 \text{ mm}$  or about 45 wall-units at the highest Reynolds number) which was found to be a good compromise between noise and filtering. Before the final pass, image deformation was also used to improve the quality of the data. Figure 2 shows a picture of the set-up.



Figure 2 : Picture of the 3C2D experiment

The high magnification 2C2D PIV cases were also analyzed with rectangular windows of  $8 \times 64$  pixels in order to increase the wall-normal resolution of the mean profile. This allows the capture of the mean gradient in the viscous sub layer in order to deduce the skin friction and then the friction velocity with an accuracy better than 1% (Willert, et al., 2018).

### 3 Results

The measurements were done at three stations in the wind tunnel at one, two and three thirds of the test section length for both PIV set-ups. The infinite velocity at the inlet of the test section was regulated at 3, 6 and 9 m/s for every cases. These locations and velocities allow nine Reynolds numbers to be obtained. A few combinations give almost the same Reynolds. The Table 1 gives the characteristics of the turbulent boundary layer for the nine Reynolds numbers obtained by the combination of results of both PIV set-ups. The friction velocity  $u_\tau$  is determined by a fit on the mean velocity profiles on the points inside the viscous sublayer.

The velocity profiles were obtained with good accuracy (noise level of both set-ups of 0.1 pixel (Cuvier & Foucaut, 2018)) and spatial resolution over the full boundary layer thickness. Figure 3 shows the mean velocity profile plotted in wall-units. For the range of Reynolds number this figure shows a good collapse in the range of  $y^+$  corresponding to the log region. This region is in agreement with the logarithmic law  $U^+ = 1/0.41 \ln(y^+) + 5.2$ . Thanks to the high magnification set-up the viscous sublayer is also very well measured.

Table 1: Boundary layer characteristics

$X(m)$	$U_e$ (m/s)	$\delta$ (cm)	$\delta^*$ (cm)	$\theta$ (cm)	$H$	$u_\tau$ (m/s)	$Re_\theta$	$Re_\tau$	$\left(\frac{\partial P}{\partial x}\right)^+$ ( $\times 10^{-4}$ )	$v/u_\tau$ (mm)
6.8	3.22	12.2	2.11	1.52	1.39	0.1268	3230	1020	-3.2	0.12
6.8	6.43	10.6	1.80	1.33	1.36	0.2375	5620	1660	-2.0	0.06
6.8	9.64	10.4	1.72	1.28	1.34	0.3456	8120	2360	-1.3	0.04
12.55	3.32	19.5	3.30	2.40	1.38	0.1224	5400	1620	-3.4	0.12
12.55	6.61	17.1	2.72	2.03	1.34	0.2352	9100	2720	-2.0	0.06
12.55	9.88	16.7	2.57	1.94	1.32	0.342	13000	3880	-1.4	0.04
19.2	3.38	27.3	4.55	3.33	1.36	0.1207	7590	2220	-3.6	0.12
19.2	6.76	24.3	3.69	2.79	1.32	0.2337	12720	3840	-2.1	0.06
<b>19.2</b>	<b>10.09</b>	<b>24.2</b>	<b>3.51</b>	<b>2.70</b>	<b>1.30</b>	<b>0.3428</b>	<b>18360</b>	<b>5590</b>	<b>-1.4</b>	<b>0.04</b>

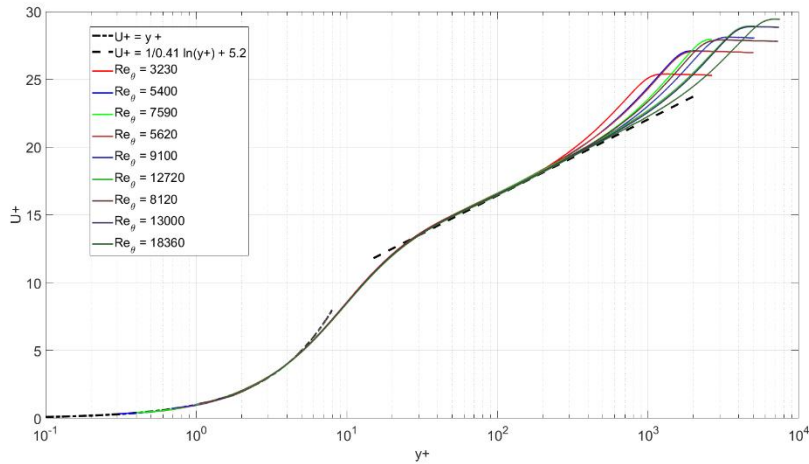


Figure 3: Mean velocity profiles in inner variable  $U^+ = f(y^+)$

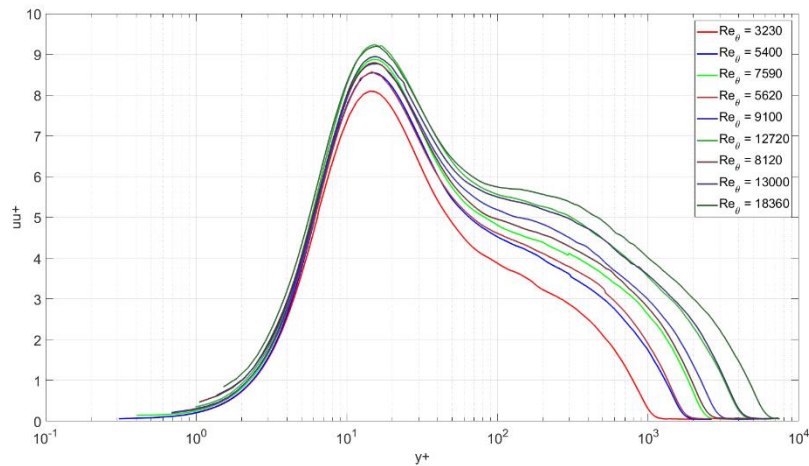


Figure 4: Streamwise Reynolds stress profiles in inner variable  $\overline{u'u'} = f(y^+)$ .

Figure 4 shows the streamwise Reynolds stress in wall units. As shown in Marusic et al. (2010) the near wall peak is located at  $y^+ = 15$  and it increases in intensity when the Reynolds number increases. A log region appears for  $y^+ > 100$  also when the Reynolds number increases.

Figure 5 shows the Reynolds shear stress in wall-units for all the range of Reynolds numbers. It shows also the plot of equation (1) which is a simplified form of the Navier Stokes equation for near wall region of TBL. This equation is classically given without pressure gradient (in black dash line in the figure). In the LMFL wind tunnel there is a slight favorable pressure gradient which can be taken into account (Table 1). Figure 5 shows also the plot of equation (1) for the highest and lowest Reynolds number cases. Even if a lack of convergence is observable in the figure, it is clear than the measurement is in good agreement with equation (1).

$$\overline{u'v'}^+ = -1 + \frac{\partial U^+}{\partial y^+} + \frac{\partial P^+}{\partial x^+} y^+ \quad (1)$$

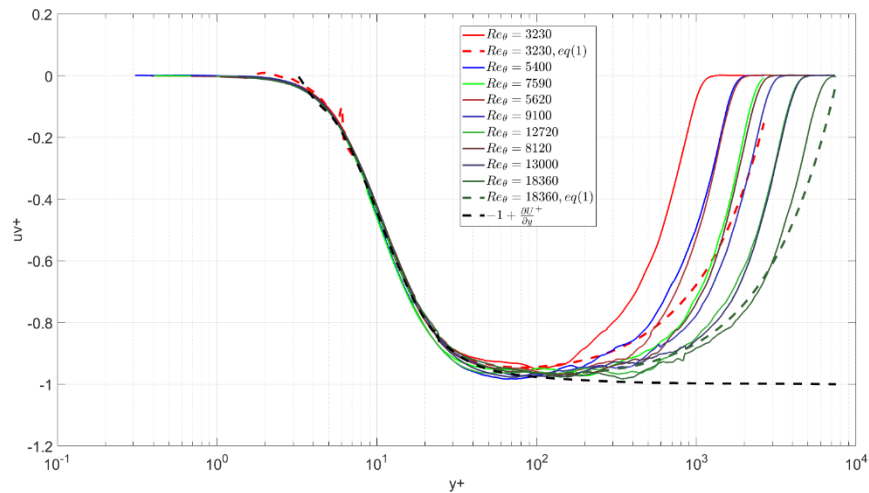


Figure 5: Reynolds shear stress profiles in inner variable  $\overline{u'v'}^+ = f(y^+)$ .

## 4 Conclusion

A full characterization of the boundary layer flow in the LMFL wind tunnel was done by means of two PIV experiments. The first experiment was carried out with a high magnification in order to capture the near wall scales and to measure the friction velocity. The second experiment was based on a double stereoscopic setup with four cameras in order to measure the full boundary layer with a good resolution. The measurement was done at three stations from the wind tunnel entrance (6.8, 12.55 and 19.2 m) and for three free-stream velocities ( $U_\infty = 3, 6$  and  $9$  m/s). Only a few results are presented here. Nevertheless, a full characterization of the boundary layer can be done for the range of Reynolds numbers obtained by playing with both distance and velocity. With an appropriate selection of the PIV magnification, better results than hot-wire measurements can be obtain, especially in the near wall region where the interrogation window of the high magnification 2C2D PIV set-ups was only 8 wall-units at the maximum Reynolds number accessible with the LMFL wind-tunnel.

## Acknowledgements

This work was carried out within the framework of the CNRS Research Foundation on Ground Transport and Mobility, in articulation with the ELSAT2020 project supported by the European Community, the French Ministry of Higher Education and Research, and the Hauts de France Regional Council.

## References

- Chauhan, K., Nagib, H. & Monkewitz, P., 2009. Criteria for assessing experiments in zero pressure gradient boundary layers.. *Fluid Dyn. Res.* 41..
- Cuvier, C. & Foucaut, J.-M., 2018. *PIV noise estimation derived from spectrum analyses*. s.l., s.n.
- Foucaut, J., Milliat, B., Perenne, N. & Stanislas, M., 2003. *Characterisation of different PIV algorithm using the europiv synthetic image generator and real images from a turbulent boundary layer*. EUROPIV2 workshop, Zaragoza, Spain, Springer.
- Klebanoff, P. & Diehl, Z., 1951. Some features of artificially thickened fully developed turbulent boundary layers with zero pressure gradient.. *Tech. Rep. 2475. DTIC Document*..
- Laval, J., Vassilicos, J., Foucaut, J. & Stanislas, M., 2017. Comparison of turbulence profiles in high-Reynolds-number turbulent boundary layers and validation of a predictive model.. *Journal of Fluid Mechanics*, 884 : R2..
- Lecordier, B. & Trinité, M., 2004. *Advanced PIV algorithms with Image Distortion Validation and Comparison using Synthetic Images of Turbulent Flow*. s.l., Proceedings of the EuroPIV 2 Workshop, March 31 - April 1, Zaragoza, pp. 115-132.
- Marusic, I. et al., 2010. Wall-bounded turbulent flows at high Reynolds numbers: Recent advances and key issues.. *Phys. Fluids* 22 (6)..
- Scarano, F., 2002. Iterative image deformation methods in PIV. *Measurement Science and Technology*, Volume 13, pp. 1-19.
- Soloff, S. M., Adrian, R. J. & Liu, Z. C., 1997. Distortion compensation for generalized stereoscopic particle image velocimetry. *Meas. Sci. and Technol.*, Volume 8, p. 1441–1454.
- Soria, J., 1998. *Multigrid approach to digital cross-correlation digital PIV and HPIV analysis*. Melbourne, 13th australasian fluid mechanics conference.
- Srinath, S. et al., 2018. Attached flow structure and streamwise energy spectra in a turbulent boundary layer. *Physical review E*, pp. 97, 053103.
- Townsend, A. A., 1976. *The structure of turbulent shear flow*. s.l.:Cambridge UP.
- Wieneke, B., 2005. Stereo-PIV using self-calibration on particle images. *Exp. In Fluids*, Volume 39, p. 267–280.
- Willert, C. et al., 2018. Experimental Evidence of Near-Wall Reverse Flow Events in a Zero. *Experimental Thermal and Fluid Science*, 91, 320:328..
- Willert, C. & Gharib, M., 1991. Digital particle image velocimetry. *Experiments in Fluids*, Volume 10, pp. 181-193.